

# Green Chemistry

Cutting-edge research for a greener sustainable future

[rsc.li/greenchem](https://rsc.li/greenchem)

Volume 23  
Number 18  
21 September 2021  
Pages 6661-7314



ISSN 1463-9262

**PAPER**

Dong Soo Hwang, Sung Yeon Hwang, Dongyeop X. Oh,  
Jeyoung Park *et al.*  
Biodegradable chito-beads replacing non-biodegradable  
microplastics for cosmetics



Cite this: *Green Chem.*, 2021, **23**, 6953

# Biodegradable chito-beads replacing non-biodegradable microplastics for cosmetics†

Sungbin Ju,<sup>a,b</sup> Giyoung Shin,<sup>a</sup> Minkyung Lee,<sup>a</sup> Jun Mo Koo,<sup>a</sup> Hyeonyeol Jeon,<sup>a</sup> Yong Sik Ok,<sup>c</sup> Dong Soo Hwang,<sup>b</sup> Sung Yeon Hwang,<sup>a,d</sup> Dongyeop X. Oh,<sup>a,d</sup> and Jeyoung Park<sup>a,b,d</sup>

The global ban on plastic microbeads for personal care products has forced researchers to find sustainable alternatives. However, current biodegradable microbeads rarely offer competitive qualities such as those related to the mechanical properties, stability, and toxicity of their degraded products. Herein, we synthesized 'chito-beads', which can satisfy the aforementioned requirements, and evaluated their practical usage, biodegradability, and phytotoxicity. Chito-beads were made into uniform spherical microbeads with a diameter of 280  $\mu\text{m}$  through the reacylation of chitosan – a renewable polymer from crustacean waste via an inverse emulsion system. Chito-beads exhibit a higher cleansing efficiency than conventional polyethylene microbeads, with a hardness of 128 MPa. Furthermore, they can be used to remove potentially toxic elements and are stable and functional in commercial cleansing. The used chito-beads were fully degraded in soils without any toxicity to the model plants. Our alternative can be used as competitive and environmentally friendly microparticles in sustainable daily necessities.

Received 6th May 2021,  
Accepted 20th July 2021

DOI: 10.1039/d1gc01588e

[rsc.li/greenchem](http://rsc.li/greenchem)

## Introduction

There is evidence that humans approximately consume a credit card worth of plastic every week by weight (Movie S1†).<sup>1,2</sup> A recent report estimated that 14 million tons of microplastics flow in the ocean annually.<sup>3,4</sup> Due to the small size of microplastics, *i.e.*, less than 5 mm long, there is no systemic method to retrieve all types of microplastics released into nature. Microplastics carry organic pollutants and are ingested by marine animals,<sup>5–7</sup> thereby moving up the food chain due to their bioaccumulation characteristics,<sup>8,9</sup> and have been found in drinking water, coastal areas, and rivers.<sup>10–13</sup> Concerns regarding the negative effects of microplastics on the human body, such as cellular damage and inflammatory and immune reactions, are increasing.<sup>14–17</sup> More importantly,

microplastic pollution is irreversible because plastics are generally non-degradable, and there are no practical means of collecting scattered microplastics in the ocean.

Microplastics are classified into two categories, primary and secondary microplastics in terms of their origin.<sup>18</sup> Natural weathering processes create secondary microplastics from macroplastic lost after use. On the other hand, primary microplastics are intentionally manufactured in small sizes. They are generally used as mechanical exfoliants for various personal care products such as toothpaste, shampoo, cleanser, and scrubs. The exfoliating particles remove dirt from the human body and are commonly made from polyethylene (PE), polypropylene, or polystyrene, owing to their suitable mechanical properties and low cost.<sup>19–21</sup> However, typically they are washed down the drains and are only minimally screened at wastewater treatment plants, thereby eventually entering the aquatic environments.<sup>22–25</sup>

Accordingly, the US has banned the use of plastic microbeads in rinse-off cosmetics on the federal level by the Microbead-Free Waters Act of 2015 (US FDA). The EU and several other countries including South Korea have also banned the use of primary microplastics in thousands of rinse-off products,<sup>26</sup> which has forced the industry to identify sustainable and biodegradable alternatives that are equivalent to exfoliating microplastics in terms of (1) cost; (2) mechanical properties; (3) solvent resistance; (4) smooth surface shape; and (5) uniform size. Three classes of biodegradable materials have been suggested as potential substitutes for cosmetics:

<sup>a</sup>Research Center for Bio-based Chemistry, Korea Research Institute of Chemical Technology (KRICT), Ulsan 44429, Republic of Korea. E-mail: crew75@kRICT.re.kr, dongyeop@kRICT.re.kr, jypark@kRICT.re.kr

<sup>b</sup>Division of Environmental Science and Engineering, Pohang University of Science and Technology (POSTECH), Pohang 37673, Republic of Korea. E-mail: dshwang@postech.ac.kr

<sup>c</sup>Korea Biochar Research Center, APRU Sustainable Waste Management Program & Division of Environmental Science and Ecological Engineering, Korea University, Seoul 02841, Republic of Korea

<sup>d</sup>Advanced Materials and Chemical Engineering, University of Science and Technology (UST), Daejeon 34113, Republic of Korea

†Electronic supplementary information (ESI) available. See DOI: 10.1039/d1gc01588e



natural hard materials (e.g., walnut shells and avocado seeds),<sup>27</sup> natural polymers (e.g., cellulose, alginate, lignin, and starch),<sup>28–31</sup> and bio-based synthesized polymers (e.g., polycaprolactone and polylactic acid);<sup>32</sup> however, all of them exhibit drawbacks. Mechanical grinding of natural hard materials results in particles with sharp edges and of irregular sizes and shapes, which scratch the surface, or may injure skin when it is used for cosmetic and rinse-off use.<sup>33</sup> Uniform sized micro-particles with smooth surfaces can be fabricated from natural and bio-based synthetic polymers by emulsifying the polymer solution.<sup>34</sup> However, the solutions that are mainly used to dissolve natural polymers, such as ionic liquids, are cost ineffective, and solution-processable biopolymers exhibit low resistance to solvents and gradually lose their mechanical properties in cosmetics that include water, oils, and surfactants. In the case of bio-based polymers such as poly(lactic acid) microbeads, processing into a uniform spherical shape is convenient, but the degradation of their ester bonds in seawater is less than 5% per year.<sup>32</sup> Thus, it is crucial for cosmetic industries to identify appropriate alternatives to microplastics.<sup>35</sup>

As a primary hard-tissue component of crustaceans, insects, and fungi, chitin is the second most abundant natural polymer that consists of *N*-acetyl-D-glucosamine repeating units. Chitin possesses great mechanical properties (stiffness of >50 GPa) and solvent resistance including both aqueous and organic solvents, owing to its highly crystalline structure.<sup>36</sup> Furthermore, it is biodegradable as well as biocompatible, and has antibacterial, antifungal, and hemostatic properties.<sup>37–39</sup> Therefore, chitin has attracted attention for use as a structural biomaterial for medical and cosmetic applications. However, the use of chitin is limited owing to processing complications related to its high crystallinity as a result of strong intermolecular hydrogen bonds. Furthermore, chitin is not readily dissolved in common solvents except for a few expensive or toxic solvents. In addition, mechanical grinding is not effective to produce chitin particles of regular size and spherical shape (Fig. S1†). For this reason, chitin is converted into chitosan with >60% of *N*-acetyl-D-glucosamine deacetylated to glucosamine. Chitosan (i.e., the deacetylated form of chitin) is solution-processable in weakly acidic solutions owing to the protonation of amine, but it loses the mechanical properties and solvent resistance of chitin due to the lower crystallinity and intermolecular hydrophobic interactions. Therefore, the physical properties of chitin and chitosan rely on the degree of acetylation, and their processability and performance are mutually exclusive.<sup>40</sup> In this regard, cytotoxic hardening agents are required to fabricate chitosan beads.<sup>41,42</sup> However, using hardening agents could slow down the degradation rate and it is difficult to estimate the toxicity of the degraded residue.

By considering the processability of chitosan and the mechanical stability of chitin, we fabricated biodegradable and biocompatible microbeads with suitable mechanical properties, solvent resistance, smooth surfaces, and regular size and shape through chitosan-to-chitin regeneration without

using cytotoxic cross-linkers. Here, we applied a facile emulsion diffusion method for producing reacylated microbeads (size: 100–500  $\mu\text{m}$ ) to replace petroleum-based microbeads. The mechanical properties, cleansing efficiency, biodegradability, and toxicity to terrestrial plants of microbeads were also assessed. Chito-beads exhibited superior properties to commercial PE microbeads especially in terms of cleansing efficiency and biodegradability, and could also adsorb potentially toxic elements (PTEs).<sup>43,44</sup> PTEs include trace elements and heavy metals such as copper, iron, and lead, which are abundant in fine dust, that can generate health risks when their concentration exceeds certain thresholds (Fig. 1). The resulting chito-beads can function as an abrasive in cosmetics and subsequently degrade in the environment without generating potential pollutants.

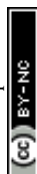
## Results and discussion

### Chito-bead preparation

Chito-beads were prepared through the reacylation of chitosan to chitin in an inverse emulsion of a chitosan aqueous solution in paraffin oil with a surfactant. Then, the emulsion particles were acetylated by acetic anhydride for 1 h at 25 °C and precipitated in an acetone/hexane/alkaline aqueous solution (Fig. 2). The particles coagulated in the alkaline solution due to deprotonation of amine, and the degree of acetylation was controlled by the acetic anhydride concentration. At mild temperature, the reacylation of amine occurred mostly with amine groups and only minimally with hydroxyl groups (Fig. 2a and b). The code name of chito-beads was CB-*N-m*, where *N* denotes the molecular weight of chitosan. There were three groups of chitosan (i.e., low-, medium-, and high-molecular weights), which are 15k, 50k–190k, and 190k–310k Da, and were denoted as L, M, and H, respectively. *m* denotes the added acetic anhydride (1.06, 3.18, and 10.6 mmol, denoted by 01, 03, and 1, respectively) during reacylation (Fig. 2c). The following chito-beads were prepared: CB-L-1, CB-M-1, CB-H-01, CB-H-03, and CB-H-1.

### Chito-bead characterization

The characteristics of the prepared chito-beads were investigated (Fig. 3). The degrees of acetylation of chitosan and reacylated chitosan were measured through conductometric titration.<sup>45</sup> The degree of acetylation of pristine chitosan was 36% and increased with the amount of acetic anhydride up to 83%; however, the molecular weight did not affect the degree of acetylation (Table 1). The Fourier-transform infrared spectroscopy (FTIR) spectra of the reacylated chitosan particles displayed no significant difference from that of commercial chitin (Fig. S2a†). The peaks of the chito-beads showed an O–H stretching vibration at 3200–3400  $\text{cm}^{-1}$  and a C–H stretching vibration at 2877  $\text{cm}^{-1}$ .<sup>46</sup> C=O and C–N stretching of amide was observed at 1634  $\text{cm}^{-1}$  and 1548  $\text{cm}^{-1}$ , respectively. However, chito-beads did not show the characteristic peaks of paraffin oil at 2851  $\text{cm}^{-1}$  and 2919  $\text{cm}^{-1}$  (C–H stretching),



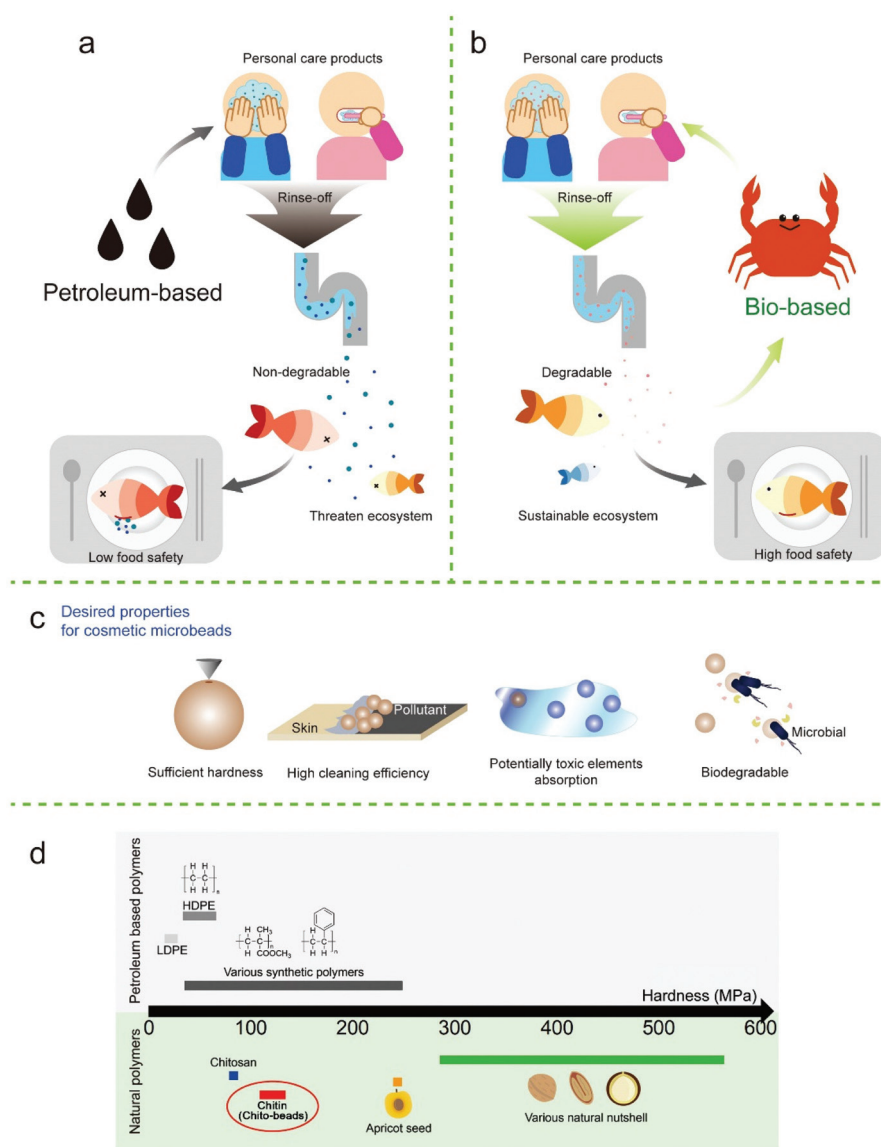


**Fig. 1** Applications of microbeads in daily care products and their potential impacts on the environment. (a) Petroleum-based microplastics and their main risks; (b) bio-based microplastics and their desired consequences for sustainable cosmetics; (c) desired cosmetic microbead properties; and (d) comparison of the hardness between the materials in this study and some natural and synthetic abrasive materials (HDPE: high-density polyethylene and LDPE: low-density polyethylene).

1456  $\text{cm}^{-1}$  (C–H bending), and 721  $\text{cm}^{-1}$  ( $\text{CH}_2$  rocking) (Fig. S2b†). This confirms that the paraffin oil was fully rinsed away.

The morphology of chito-beads was observed using an optical microscope and a scanning electron microscope (SEM) (Fig. 3a–c; Fig. S3†). In the emulsion-based particle fabrication system, the ratio between the continuous and dispersion phases, stirring speed, and the amount of surfactant mostly affected the particle morphology and size.<sup>47</sup> The diameters of CB-L-1, CB-M-1, and CB-H-1 were 140, 260, and 280  $\mu\text{m}$ , respectively. As the viscosity of chitosan solution changes with the molecular weight, CB-L-1 showed the smallest particle size. CB-H-01 was larger (370  $\mu\text{m}$ ) than CB-H-03 and CB-H-1 due to

the high intermolecular attraction which leads to aggregation while stirring.

It was easy to fabricate colored chito-beads. In the same manner, chito-beads were fabricated through the acetylation of chitosan in the inverse emulsion after red, green, and blue dyes, used for food coloring, were dissolved in the chitosan aqueous solution at a concentration of 4  $\text{mg mL}^{-1}$ . Fig. 3d shows the chitosan solutions prepared with red, green, and blue dyes, and the resultant vividly colored chito-beads.

Water-resistance of microbeads under aqueous conditions is important because water-based personal care products are most common on the market. Swelling and dissolution resistance are functions of water resistance.<sup>39</sup> The swelling ratio of



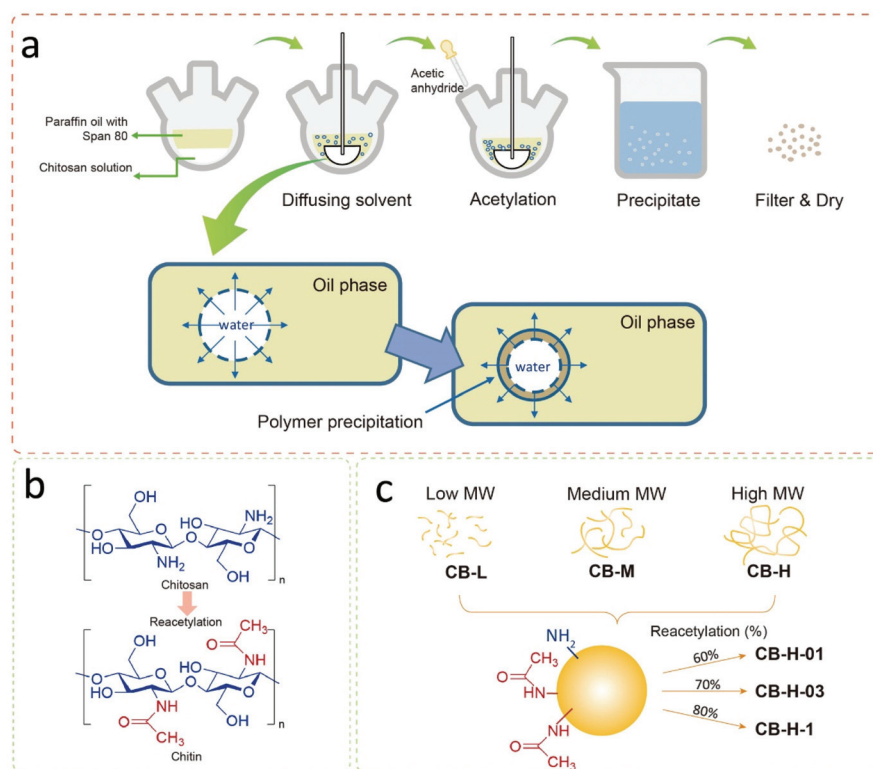


**Fig. 2** Chito-bead preparation. (a) Schematic illustration of chito-bead preparation via the emulsion diffusion method; (b) chemical structures of chitosan and chitin when acetylated under mild conditions; and (c) depiction of the prepared chito-beads with various molecular weights (MWs) and reacylation degrees.

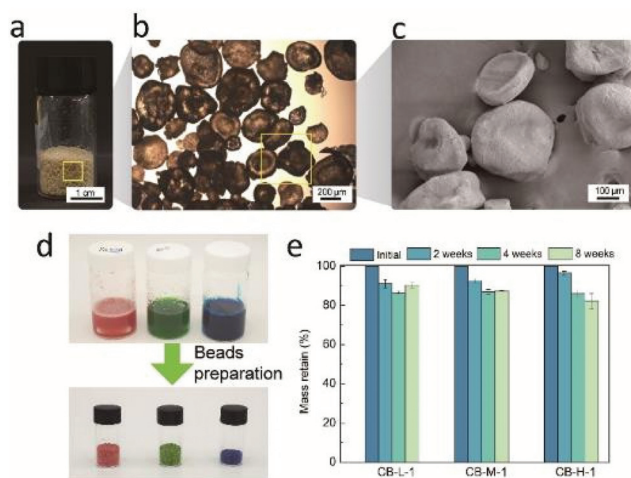


**Fig. 3** Chito-bead characterization. (a) Photograph, (b) optical microscopy, and (c) SEM images of CB-H-1; (d) photograph of colored chitosan solutions and chito-beads made with colored solution; and (e) mass retained in sterilized deionized water for 2, 4, and 8 weeks under ambient conditions compared with the molecular weight of chito-beads. Error bars represent the standard deviation ( $n = 3$ ).

each particle was measured by the weight change of the particle after immersion in distilled water for 3 days. The swelling ratio of chito-beads decreased from  $9.6 \text{ g g}^{-1}$  to  $2.7 \text{ g g}^{-1}$  when

the degree of acetylation increased from 60% to 83% (Table 1), due to the acetyl amide group of chitin being more hydrophobic than the amine of chitosan. On the other hand, the swelling ratio was independent of the molecular weight. The swelling ratios of chito-beads were as low as those reported for chitin and chitosan particles ( $1.5$  to  $12 \text{ g g}^{-1}$ ), which were synthesized with cross-linkers and hydrophobic additives.<sup>48,49</sup>

Weight loss during water immersion is an indicator of dissolution resistance. Chito-beads with different molecular weights were immersed in sterilized distilled water for 2, 4, or 8 weeks. CB-L-1 and CB-M-1 had lower molecular weights than CB-H-1. Thus, CB-H-1 presented a lower weight loss (3.6%) during immersion than CB-L-1 (7.5%) and CB-M-1 (8.9%) after 2 weeks (Fig. 3e). After 8 weeks, the weight loss of chito-beads in water was approximately 15%. In comparison to the group with the same molecular weight but different degrees of acetylation (%), CB-H-01 showed a notably high weight loss of 19% in 2 weeks due to the low degree of acetylation (Table 1).

In addition, the shape of CB-H-01 was deformed upon drying after 2 weeks of swelling (Fig. S4†). The high degree of swelling in the aqueous environment was mainly attributed to the high proportion of hydrophilic amine groups remaining in the CB-H-01. The  $\text{pK}_a$  of the primary amine of chitosan is  $\sim 6.5$ , which contributes to the solubility of chitosan in acidic pH. However, chitosan with an acetylation degree below 60% can



**Table 1** Characterization of acetylated chitosan particles in terms of their molecular weight and degree of acetylation

Sample code	Molecular weight of chitosan (kDa)	Chitosan solution concentration (%)	Degree of acetylation <sup>a</sup> (%)	Size <sup>b</sup> (μm)	Swelling ratio <sup>c</sup> (g g <sup>-1</sup> )	Mass retained after 2 weeks <sup>d</sup> (%)
CB-L-1	15	2	80	140 (±60)	2.8 (±0.7)	92.5
CB-M-1	50–190	2	83	260 (±110)	3.2 (±0.8)	91.1
CB-H-1	190–310	2	83	280 (±110)	2.7 (±0.5)	96.4
CB-H-03	190–310	2	72	230 (±80)	6.6 (±0.8)	94.9
CB-H-01	190–310	2	60	370 (±100)	9.6 (±1.0)	80.9

<sup>a</sup> Calculated through conductometric titration. <sup>b</sup> Averaged mean value (±standard deviation) from more than 150 measurements obtained using an optical microscope. <sup>c</sup> Mass ratio of the swollen water weight to the dry weight of particles. <sup>d</sup> Percent mass remaining after 2 weeks in deionized water.

also be dissolved in neutral pH, driven by dipole–dipole and ion–dipole interactions with water molecules.<sup>50,51</sup>

On the other hand, CB-H-1 particles maintained their spherical shapes and were not easily deformed under wet conditions because the reacylated group was minimally hydrated differently from chitosan.

Mechanical exfoliation and abrasion performances of particles mainly rely on their mechanical properties. Particles should be hard enough to remove contaminants without damaging human tissues. The mechanical properties of chitin depend on the degree of acetylation, and the hardness is no exception. To evaluate the hardness of chito-beads, chitin films with the same degree of acetylation were prepared by solvent casting with the same molecular weight used for preparing chito-beads. Hardness was determined through a nano-indentation technique as per the ASTM E2546 standard. The hardness was higher in chitin than in chitosan, which has a higher degree of acetylation, but was less dependent on the molecular weight. CB-L-1, CB-M-1, and CB-H-1 films showed similar hardnesses of 130, 113, and 128 MPa, respectively, while the chitosan film exhibited a low hardness of 83 MPa. The hardness of chito-beads was compared to that of the materials used as skin exfoliators such as nutshells, apricot seeds, and plastics (Fig. 1d; Table S1†). The hardness values of synthetic plastics ranged from 20–250 MPa,<sup>52–56</sup> and those of nutshells and apricot seeds were >244 MPa.<sup>54,57</sup> Therefore, the chito-beads produced in this work exhibited an appropriate hardness for application as cosmetic microbeads.

### Chito-bead cleansing efficiency

To use chito-beads as daily care abrasives, it is essential to investigate their practical cleansing efficiency on the skin. Accordingly, the inner forearm and back of the hand were selected as the substrates because they are flat and hairless. A waterproof eyeliner was used to mimic a pollutant on the skin. A cosmetic cleanser was fabricated by mixing 4 mL of liquid soap and 50 mg of PE microbeads or CB-H-1. The PE microbeads were separated from a commercial cosmetic cleanser, and the ingredients of the liquid soap have been described in the ESI (Table S2†). The CB-H-1 cleanser exhibited more rapid pollutant removal than that achieved by using the PE microbead cleansers or the liquid soap, regardless of their shape (Fig. S5 and S6; Movie S2†). This is attributed to the

spherical and regular shaped CB-H-1 particles demonstrating balanced exfoliation compared to that observed with irregularly shaped PE microbeads (Fig. S7†), and to the amine group on CB-H-1 exhibiting a higher affinity for the pollutant than for PE (with only hydrocarbon chains). As the sole natural cationic polysaccharide, chitosan has great potential in wastewater treatment because its amine and hydroxyl groups act as adsorption sites for heavy metal ions and anionic organic pollutants.<sup>58,59</sup>

A solid type cleanser (Fig. 4a) was fabricated with a combination of solid soap (1 cm<sup>3</sup>) and CB-H-1 (50 mg) because solid soap could provide balanced force when cleaning compared to liquid soap. The pollutant was removed with solid soap and solid type cleansers under identical force by using a sharp wooden stick (Fig. 4b; Movie S3†). The solid cleanser with CB-H-1 presented a cleansing rate that was four times faster than that provided by solid soap, which shows better cleansing efficiency; these observations are consistent with the results of the liquid soap tests. Compared with the control, it can be seen that pollutants were removed much more rapidly when the beads were present. When the cleansing agent contained microbeads, friction was generated while rubbing, which increased the cleansing efficiency. Mechanical friction not only physically removed contaminants but also increased the interaction between the cleansing agent and the pollutant to ensure higher removal efficiency.

We also investigated the cleansing effect of chito-beads on a waterproof sunblock composition. The sunblock was applied to porcine skin. Under a 365 nm UV light, extinguished fluorescence (*i.e.*, dark color) indicated that the porcine skin was thoroughly covered with sunblock. Then, the porcine skins were cleansed for 30 s with water in the presence or absence of solid soap only, or by using solid soap with chito-beads. As seen in Fig. 4c, some sunblock remained even after being cleansed without soap only, whereas cleansing with soap and chito-beads resulted in the noticeable removal of sunblock. The cleansed area (%) was calculated using ImageJ software by setting the sunblock applied area as 100%. The cleansed area of the samples treated with both soap and chito-beads was 68.2%, while the cleansed areas of the samples treated with soap without chito-beads, and with water only, were 39% and 0% respectively. This outcome is consistent with the previous pollutant removal simulations, and the results suggest that



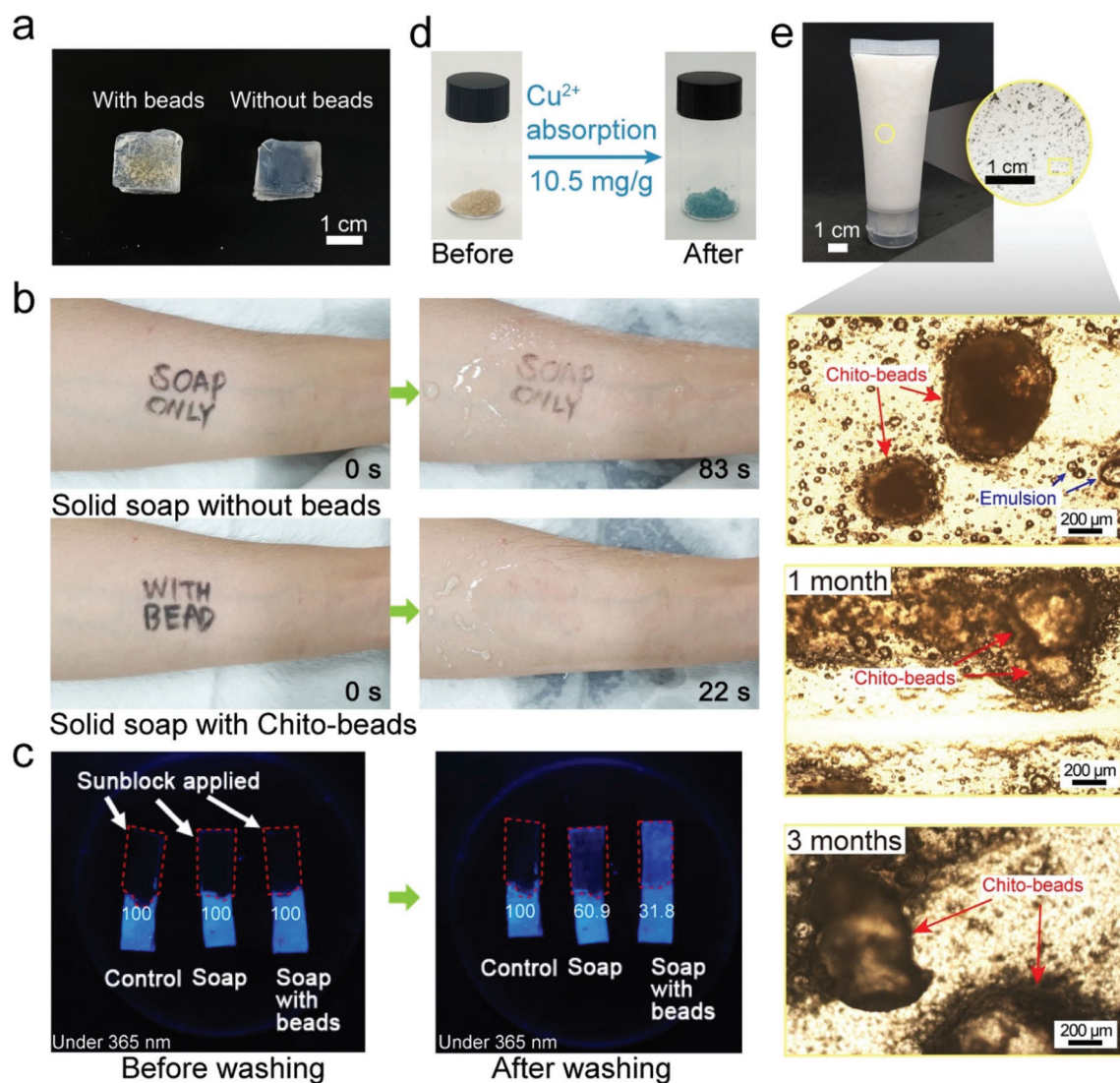


**Fig. 4** Cleansing efficiency test of chito-beads. (a) Photograph of solid soap with and without CB-H-1, and comparison of their cleansing efficiency (b) on the skin and (c) sunblock on porcine skin, where the numbers denote the percentage of sunblock applied; (d) copper(II) absorption capacity of CB-H-1; and (e) photograph of a skin exfoliator product including chito-beads and magnified optical microscopy images of the cleanser content with time lapse.

acetylated chitosan microbeads have good potential for use as an abrasive and as a substitute for existing commercial petroleum-based microplastics.

It is a well-known fact that chitin has the ability to remove PTEs from aqueous solutions. Chitin can chelate with cations by means of the lone pair electrons of nitrogen in the acetamido/amino group.<sup>60</sup> Absorption capacity ( $\text{mg g}^{-1}$ ) is defined as the quantity of the cations chelated by the chitobeads of unit weight. After CB-H-1 was incubated in an aqueous solution with 1000 ppm Cu, a PTE, at pH 5.5 for 24 h, the CB-H-1 particles turned bluish hues (Fig. 4d). The adsorption capacity for Cu was  $10.5 \text{ mg g}^{-1}$ . This ability shows the potential to help users cleanse their skins of fine dust containing PTEs.<sup>61</sup> After the cleansing efficiency of chito-beads was confirmed, their stability in the existing product was assessed. A commer-

cial face cleanser (25 mL) was mixed with 5 wt% chito-beads and placed into a small tube. Chito-beads maintained their shape in facial cleanser or even in paraffin oil (Fig. 4e; Fig. S8†).

#### Chito-bead biodegradability

Microplastics are typically single-use and are washed out into the sewage system. It is not economically feasible to install a high-performance membrane that rejects microplastics in sinks and sewage treatment plants; hence, microplastics flow directly into downstream or coastal water areas. Therefore, it is important to investigate the biodegradability of the newly developed microbeads. Chitin is naturally degraded by micro-organism enzymes, and many studies have been conducted on chitinases, *i.e.*, enzymes that degrade chitin.<sup>62</sup> First, we exam-

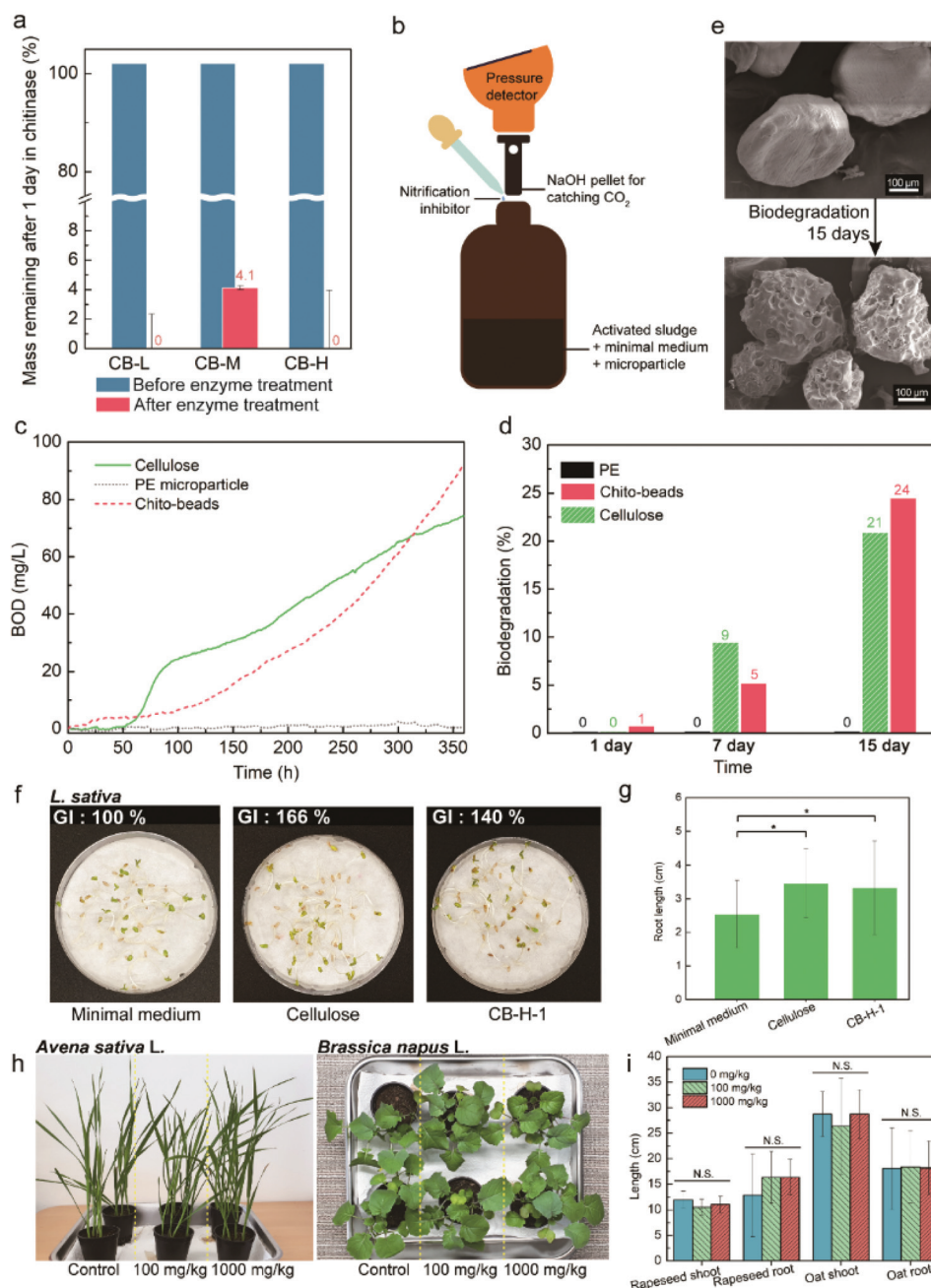


**Fig. 5** Chito-bead biodegradability. (a) Comparison of percent mass of chito-beads remaining after 1 day of incubation in chitinase. (b) Schematic illustration of the closed respirometer measured for BOD. Comparison of biodegradability between CB-H-1, commercial PE microbeads and cellulose (c) in BOD and (d) biodegradability calculated from ThOD. (e) SEM image of chito-beads before and after biodegradation. (f) Representative sample and the GI of germinated *Lactuca sativa* seeds treated with the minimal medium, and the solution after the BOD test. (g) Root lengths of germinated seeds grown for 5 days. Statistical analysis was performed using Student's *t*-test ( $n = 180$ ). \* indicates a significant difference ( $P < 0.05$ ). Error bars represent the standard deviation. (h) Photographs of oat (*Avena sativa* L.) and rapeseed (*Brassica napus* L.) grown in soils mixed with chito-beads ( $0 \text{ mg kg}^{-1}$  [control],  $100 \text{ mg kg}^{-1}$ , and  $1000 \text{ mg kg}^{-1}$ ). (i) Comparison of mean shoot and root lengths after 14 days of growth. Statistical analysis was performed using Student's *t*-test ( $n = 10$ ); n.s. refers to not significant. Error bars represent the standard error.

ined chito-bead degradation by chitinase. Chito-beads were incubated in a phosphate-buffered saline (PBS) solution containing chitinase for 24 h at 37 °C and passed through filter paper. Then, the residue on filter paper was analyzed. As expected, chito-beads were totally decomposed into an invis-

ible level. The weight change indicated that >95% of chito-beads were hydrolyzed into indistinguishable molecules (Fig. 5a).

Aerobic biodegradation occurs when microorganisms consume organic matter and oxygen and ultimately produce



carbon dioxide, water, and biomass. Thus, the biochemical oxygen demand (BOD) of a sample is a measure of the degree of biodegradation. BOD was measured by the oxygen repository test referring to ISO 14851 with a closed system, as shown in Fig. 5b. The sample was incubated in a closed bottle after activated sludge from a sewage treatment plant was added (Fig. S9†). Biodegradability (%) is expressed by the ratio of BOD and theoretical oxygen demand (ThOD). The results of chito-beads were compared with cellulose and PE particles, which are representative of biodegradable and non-degradable materials, respectively (Fig. 5c). After 15 days, the biodegradabilities of CB-H-1 and cellulose were 24% and 20%, respectively, while that of PE was negligible (Fig. 5d). The smooth surface of pristine CB-H-1 became porous (Fig. 5e). The data suggest that microorganisms metabolized chito-beads. If natural features of chitin were well regenerated during chitosan reacylation, chito-beads could degrade in seawater. After 1 month of soaking chito-beads in seawater, 93.2% of the chito-beads degraded, while PE microbeads of commercial products did not (Fig. S10†). Since soil microplastics research began, there has been an understandable interest in figuring out whether these small plastic particles can be absorbed onto plants and, eventually, into the food we eat.<sup>63</sup> Therefore, microbead and its degradation products should not have negative effects on soils and plants.<sup>64</sup> To further test the phytotoxicity of chito-beads and their degradation products, we studied lettuce (*Lactuca sativa*) seed germination in the residual aqueous solution after the BOD test. As shown in Fig. 5f, lettuce (*Lactuca sativa*) seeds were cultivated in wet cotton at 25 °C under 85% relative humidity (RH) for 5 d. Root lengths >2 cm were considered as germination. The minimal medium was a negative control because it was used as the background solution for the BOD test. The degradation product of chito-beads exhibited a positive effect on lettuce root growth. The root germination rates with the degradation products of chito-beads, cellulose, and the negative control were 77%, 87%, and 72%, respectively, and the mean root lengths were 3.3, 3.5, and 2.5 cm, respectively (Fig. 5g). The germination index (GI) was calculated as: (number of germinated seeds in the sample/number of germinated seeds in the control) × (mean root length of seedlings in the sample/mean root length of seedlings in the control) × 100.<sup>65</sup> In comparison with the minimal medium, the GI values of solutions containing chito-beads and cellulose degradation products are 140.2% and 165.7%, respectively, which indicates superior lettuce seed germination (Fig. 5f). Degraded chitosan is known to have a positive effect on GI and plant growth, making it a potential growth promoter for agriculture purposes.<sup>66,67</sup> Also, it is a representative natural polysaccharide degradation product.<sup>68</sup>

The seedling growth tests with oat and oilseed rape were conducted with chito-beads. We investigated the influences of chito-beads on the germination and growth of oat (*Avena sativa* L.) and rapeseed (*Brassica napus* L.) in soils by referring to the OECD 208: terrestrial plant test. Chito-beads were mixed with soil at concentrations of 100 or 1000 mg kg<sup>-1</sup>. Then, five seeds were planted in 75 g of soils in a flower pot (Fig. S11a†), and

seedlings were grown for 14 d after germination. Both plant types grew well regardless of the chito-bead concentration (Fig. 5h). Plant germination, growth, and productivity were quantitatively analyzed from the germination rate, seedling dry weight, seedling vigor index (SVI), and root and shoot lengths (Fig. 5i; Fig. S11b and S11c; Tables S3 and S4†). SVI-I and -II were calculated as: (seedling length × germination rate) and (seedling dry weight × germination rate), respectively.<sup>69</sup> There was no significant difference between the soils mixed with a high chito-bead concentration and the control ( $p > 0.05$ ) with respect to germination and growth of either oat or rapeseed because the degradation product of chito-beads did not significantly affect the organic matter. The above results show that chito-beads degraded well in the presence of chitinase, microorganisms from wastewater plants, and seawater. The degraded product improved plant germination and the solid beads had a minimal negative effect on soils.

## Conclusions

In this study, we reported the use of cheap, abundant, and sustainable microplastics in the form of microbeads to replace non-degradable skin exfoliators. Chitin microbeads were prepared through reacylation of chitosan in a water-in-oil inverse emulsion system. The size and shape of the particles were governed by the molecular weight and the degree of acetylation, which was in contrast to natural chitin; however, the microbeads presented analogous features with neat chitin in terms of physical properties and environmental effects. They achieved adequate hardness to remove pollutants without damaging the skin. As a result, they showed higher cleansing efficiencies than commercial PE microbeads. Chito-beads absorbed PTEs and organic pollutants owing to their acetyl amide groups, and were degraded by enzymes, microorganisms, and seawater. The degradation product exhibited positive effects on plant germination and growth. This study presents a method for producing chitin particles without the use of toxic or expensive organic solvents, resulting in the production of cost-effective and environment friendly microbeads. Chito-beads could provide a new alternative product that will mitigate the environmental problems caused by cosmetic microplastics, and achieve the United Nations' Sustainable Development Goals (SDG6: clean water and sanitation, SDG14: life below water, and SDG15: life on land).

## Experimental

### Materials

Chitosan (15 kDa [low-molecular weight]) was purchased from Polyscience, Inc. (USA). Chitosan (50–190 kDa [medium-molecular weight] and 190–310 kDa [high-molecular weight]), sorbitan monooleate (Span® 80), acetic anhydride (≥98%), M9, mineral salts, and Chitinase from *Streptomyces griseus* were



purchased from Sigma-Aldrich (USA). Acetic acid (99.5%) and paraffin oil were purchased from Samchun (Korea).

### Chito-bead preparation

The procedure for preparing CB-H-1 is described as follows. Chitosan (190–310 kDa, 0.5 g) was added to 0.1 M acetic acid (25 mL) and stirred until homogeneously dissolved. Span® 80 (12.5 mg, 2.5% of the solute) was added into paraffin oil (100 mL), and the solution was placed in a round-bottomed flask. While stirring at 400 rpm with an overhead stirrer, the prepared chitosan solution was injected through a 25 mL syringe. After 3 h of vigorous stirring, acetic anhydride (1 mL, 10.6 mmol) was mixed with methanol (1 mL) and slowly added dropwise to the reactor. After stirring for an additional 1 h for acetylation, the solution was poured into a mixture of hexane and ethanol (1 L; 1/1 v/v) and was stirred with 1 M NaOH (2.5 mL). The solution was filtered through qualitative filter paper (Advantec No. 2, Japan, pore size = 5 µm), and washed with hexane and acetone several times to remove residual oil. Sample particles were dried in a vacuum oven at 60 °C overnight and characterized using Fourier transform infrared spectra (FTIR, Nicolet iS50, Thermo Fisher Scientific Co., USA). FTIR: 3200–3400 cm<sup>-1</sup> (O–H stretching), 2873 cm<sup>-1</sup> (C–H stretching), 1652 cm<sup>-1</sup> (amide I), and 1558 cm<sup>-1</sup> (amide II). In addition, CB-L-1 and CB-M-1 were prepared with chitosan, having a molecular weight of 15 kDa and 50–190 kDa.

### Chito-bead characterization

The morphology of each sample was determined using an optical microscope (Zeiss Axio Imager A2m, Germany) and a scanning electron microscope (SEM, JSM-6010LV, JEOL, Japan).

The size distribution of the prepared particles was determined by measuring 150 random particles using an optical microscope and calculating the mean size and the standard deviation. In order to obtain the swelling ratio, the particles (0.05 g) were introduced in distilled water (5 mL) at 25 °C for 3 days. When fully swollen, the particles were taken out and tapped with filter paper to remove the remaining water. The swollen particles were weighed and the swelling ratio was calculated using eqn (1) as follows:

$$\text{Swelling ratio (g g}^{-1}\text{)} = (W_s - W_d)/W_d \quad (1)$$

where  $W_s$  indicates the weight of swollen particles and  $W_d$  is the dried weight of particles. The measurement of the swelling ratio was performed in triplicate.

In the water stability test, each particle (50 mg) was sterilized at 121 °C for 1 h and placed in distilled water (5 mL) at 25 °C. After 2, 4 and 8 weeks, the particles were removed and dried in a vacuum oven at 50 °C for 3 days to completely remove residual water. Dried particles were weighed and water stability was calculated using eqn (2) as follows:

$$\text{Water stability (\%)} = W_n/W_0 \times 100 \quad (2)$$

where  $W_n$  denotes the weight of dried particles after  $n$  days and  $W_0$  is the initial weight of particles. All samples were triplicated.

The hardness of each sample (depending on the molecular weight) was measured in the form of a film, which was prepared as follows: (1) chitosan aqueous solution was acetylated with acetic anhydride according to the same procedure for preparing chito-beads and (2) reacylated chitosan solution was solution-cast and dried at 25 °C for 1 week to prepare the film. The hardness was evaluated using a nanoindentation tester (UNHT, Anton Paar) with a Berkovich tip. The maximum indentation load was 50 mN with a loading rate of 100 mN min<sup>-1</sup>. Each sample was tested at three points, and the mean and standard deviations were calculated.

### Conductometric titration of chito-beads

The degree of acetylation of particles was determined by conductometric titration. This analysis was performed with a pH meter (Orion Star A211, Thermo Scientific) and a conductometer (912 Conductometer, Metrohm). Reacylated chitosan particles (50 mg) were submerged in 0.01 M HCl solution (15 mL) and stirred for 1 day to protonate the remaining amine groups of chitosan. After protonation of reacylated chitosan particles, 0.025 M NaOH solution was added dropwise at a rate of 0.05 mL min<sup>-1</sup> using a syringe pump (Legato 200, KD Scientific) until the pH of the solution reached 11.0. The degree of acetylation (%) was calculated using eqn (3) as follows:

$$\text{Degree of acetylation (\%)} = \left(1 - \frac{[\text{base}](V_2 - V_1)161}{m}\right) \times 100 \quad (3)$$

where [base] refers to the concentration of the NaOH solution (in mol L<sup>-1</sup>);  $V_1$  and  $V_2$  are the volumes of NaOH (mL) used in the titration (*i.e.*, the volumes of NaOH required to neutralize the ammonium groups of chitosan); 161 is the molar mass of the chitosan monomer; and  $m$  is the dry mass of the sample (mg).

### Extraction of microbeads from a commercial skin exfoliator

As a control, PE microbeads were extracted from a commercial skin exfoliator from L'Oréal Paris Body Sublime (bought in 2014). The gel scrub (10 mL) was submerged in ethanol and stirred vigorously for 24 h to dissolve other materials. The solution was filtered through filter paper (Advantec No. 2, Japan, pore size = 5 µm) and rinsed thoroughly with ethanol and distilled water. The obtained white PE particles were dried overnight at 50 °C under vacuum, and FTIR was used to confirm their characteristics.

### Chito-bead cleansing efficiency

Cleansing efficiency tests were carried out on the inner arm, back of the hand, and porcine skin. Commercially available waterproof eyeliners and sunblock were used to simulate real-life use. First, after applying waterproof eyeliner on the skin, PE microbeads (50 mg) and chito-beads (50 mg) were added to



liquid soap (Joong Il Oil Chemical Co., Korea) and rubbed constantly by hand. In addition, solid soap (Joong Il Oil Chemical Co., Korea) size of 1 cm<sup>3</sup> was prepared with and without chito-beads (50 mg).

For the sunscreen removal test, sunscreen was applied on porcine skin (1 × 4 cm<sup>2</sup>) and 365 nm UV light was used to confirm whether the skin was fully covered. Then, as a control, porcine skin was washed under flowing water for 30 s; as an experiment, soap and soap with added chito-beads (50 mg) were subsequently rubbed for 30 s. Finally, the porcine skin was gently washed with water and patted lightly. The sunscreen removed from porcine skin was monitored under a 365 nm UV light. Then, the images were analyzed using ImageJ software to quantify the area that was cleaned. The images were processed as 8-bit images with fixed thresholds of 43–255. The area (%) was calculated by dividing the processed area by the original porcine skin area.

### Potentially toxic element absorption properties of chito-beads

Potentially toxic element (PTE) absorption was assessed using 1000 ppm stock solutions of copper ions. Copper(II) nitrate was dissolved in distilled water to prepare stock solutions (1 Cu<sup>2+</sup>-mg L<sup>-1</sup> = 1000 ppm). Dried CB-H-1 particles (50 mg) were added to the 1000 ppm solution, followed by stirring at room temperature for 24 h to allow complete absorption of PTE. The remaining solution was filtered with a 0.45 µm polyvinylidene difluoride syringe filter, and PTE concentration was measured using an ICP-OES (iCAP 6000, Thermo Scientific). The PTE absorption capacity (A) was calculated using eqn (4) as follows:

$$\begin{aligned} \text{PTE(copper)absorption capacity(A)} \\ = (C_0 - C_e) \frac{V}{m} (\text{mg g}^{-1}) \end{aligned} \quad (4)$$

where  $m$  (g) is the dry weight of chito-bead particles;  $V$  (L) is the volume of the copper ion solution; and  $C_0$  and  $C_e$  (mg L<sup>-1</sup>) are the initial and equilibrium copper ion concentrations, respectively.

### Enzymatic degradation of chito-beads

Enzymatic degradation of chito-beads was investigated using chitinase from *Streptomyces griseus*. Chito-beads (10 mg) were soaked in phosphate-buffered saline (PBS) solution (3 mL, pH 7.4). Then, 2 units of chitinase were added into a shaking incubator and incubated for 24 h at 37 °C. Subsequently, the incubated beads were filtered through a 0.45 µm polytetrafluoroethylene (PTFE) membrane and washed thoroughly with distilled water. The washed beads were dried in a vacuum oven at 60 °C overnight and were then weighed.

### Degradation study

The biodegradation properties of chito-beads were measured by respirometry methods using the modified ISO 14851 method by calculating the biochemical oxygen demand (BOD) from the measured pressure change by the amount of oxygen consumed in the closed bottle. The pressure change was determined using OxiTop® (WTW, Germany), and the bio-

degrading medium was prepared as follows: a minimal medium was prepared by mixing M9 solution (10 mL, containing KH<sub>2</sub>PO<sub>4</sub>, NaCl, Na<sub>2</sub>HPO<sub>4</sub>, and NH<sub>4</sub>Cl), 0.09 M MgSO<sub>4</sub>·7H<sub>2</sub>O, 0.25 M CaCl<sub>2</sub>·2H<sub>2</sub>O, 0.9 mM FeCl<sub>3</sub>·6H<sub>2</sub>O (1 mL each), and distilled water (1 L). Solid activated sludge from an aeration tank (0.5 g) was introduced into distilled water (500 mL), homogenized for 2 min, and left for 30 min to allow the solids to precipitate. Subsequently, 8.2 mL of the supernatant of the sludge solution was collected and mixed with 155.8 mL of the minimal medium in each closed respirometer. Chito-beads (50 mg) and PE microbeads (50 mg) were tested for 15 days at 20 °C. All tests were performed in duplicate.

Theoretical oxygen demand (ThOD) of material C<sub>c</sub>H<sub>h</sub>O<sub>o</sub>Cl<sub>cl</sub>N<sub>n</sub>S<sub>s</sub>P<sub>p</sub>Na<sub>na</sub>, the molecular weight of whose repeating unit is  $M_r$ , was calculated using eqn (5) as follows:

$$\text{ThOD} = \frac{16[2c + 0.5(h - cl - 3n) + 3s + 2.5p + 0.5na - o]}{M_r} \quad (5)$$

Biodegradation (%) was calculated from the measured BOD compared with ThOD using eqn (6) as follows:

$$\text{Biodegradability (\%)} = \text{BOD/ThOD} \times 100. \quad (6)$$

The degradation in the seawater study was conducted in an aquarium (95 × 70 × 55 cm<sup>3</sup>) which houses live fish (*G. punctata*) and is maintained at 20 (±2) °C. The samples were placed inside 85-denier nylon tights through which particles cannot penetrate. PE microbeads were used as a negative control. After 1 month, the tights were removed and the particles remaining in the tights were filtered through 0.45 µm PTFE membranes and dried in a vacuum oven at 50 °C before the dried particle mass was measured.

### Phytotoxicity study

Phytotoxicity of the microbeads was tested using non-treated *L. sativa* seeds with a germination rate >85%. The seeds were washed with distilled water prior to testing. The sample solutions from the oxygen respirometric test were used for testing phytotoxicity after filtration. The filtrate (as a sample) and the minimal medium (as a control; 5 mL) were placed in a Petri dish with clean filter paper (Whatman, No. 2). Thereafter, 30 seeds were placed on the filter paper, covered with a lid, and incubated for 5 days at 25 °C and a relative humidity of 85%. The root lengths of germinated shoots were measured. For calculation of the germination rate, the shoots with roots longer than 2 cm were counted. The germination rate and GI were calculated using eqn (7) and (8) as follows:

$$\text{Germination rate(\%)} = \frac{(\text{Number of germinated seeds})}{(\text{Total number of seeds})} \times 100 \quad (7)$$

$$\text{Germination index (\%)} = (G_s/G_c) \times (L_s/L_c) \times 100 \quad (8)$$

where  $G_s$  and  $G_c$  indicate the number of germinated seeds in the sample and in the control, respectively and  $L_s$  and  $L_c$  denote the



mean root lengths of the sample and the control, respectively. In addition, the mean and standard deviation of root lengths were calculated and the significance of each sample was verified through *t*-tests. The experiments were repeated six times.

In order to evaluate the phytotoxicity of the solid microbead substance on germination and early growth of terrestrial plants, the test was conducted referring to the OECD 208. The plants used in the test were oat (*Avena sativa* L.) and oilseed rape (*Brassica napus* L.), and the seeds were supplied by a private company (Chungnong, Korea). Base soil was passed through a 500  $\mu\text{m}$  sieve and mixed with chito-beads to concentrations of 0  $\text{mg kg}^{-1}$ , 100  $\text{mg kg}^{-1}$ , and 1000  $\text{mg kg}^{-1}$ . The detailed characterization of the soil batch is described in Table S5.† Control and mixed soils were placed in disposable plastic pots without any treatment and the seeds were planted 1–2.5 cm below the surface. Plants were cultured under a 16/8 light/dark photoperiod (30–36 K lux) at 20 °C with 75% relative humidity and the experiment was terminated 14 days after germination of 50% of the control. Plant lengths were measured directly after reaping the plants and the dry masses were measured after drying the plants in the oven at 70 °C for 3 days. The seedling vigor index was calculated using eqn (9) as follows:

$$\text{Seedling vigor index I} = \text{Germination rate}(\%) \times \text{mean seedling length}(\text{cm}). \quad (9)$$

In addition, the seedling vigor index was also calculated in terms of dry weight using eqn (10) as follows:

$$\text{Seedling vigor index II} = \text{Germination rate}(\%) \times \text{mean seedling dry weight}(\text{g}). \quad (10)$$

### Statement of compliance

All experiments involving human participants were in accordance with the ethical standards of the National Research Committee and with the 1964 Helsinki Declaration and its later amendments or comparable ethical standards. Informed consent was obtained from all the participants. Consents for publishing the results of the experiments have been taken from all the participants. The privacy of the participants has been maintained and absolute confidentiality has been guaranteed.

### Author contributions

S. J., G. S., and M. L. performed the experiments. J. M. K., H. J., and Y. S. O. analysed the data. S. J., D. X. O., and J. P. prepared the figures and wrote the paper. D. S. H., S. Y. H., D. X. O., and J. P. conceived, designed, and directed the project. All authors have given approval to the final version of the manuscript.

### Conflicts of interest

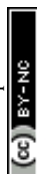
There are no conflicts to declare.

### Acknowledgements

This research was supported by KRICT (Core Project; SS2142-10), the Bio-Industrial Technology Development Program (20008628) funded by the Ministry of Trade, Industry and Energy (MI, Korea).

### Notes and references

- 1 R. Geyer, J. R. Jambeck and K. L. Law, *Sci. Adv.*, 2017, **3**, e1700782.
- 2 S. B. Borrelle, J. Ringma, K. L. Law, C. C. Monnahan, L. Lebreton, A. McGivern, E. Murphy, J. Jambeck, G. H. Leonard, M. A. Hilleary, M. Eriksen, H. P. Possingham, H. De Frond, L. R. Gerber, B. Polidoro, A. Tahir, M. Bernard, N. Mallos, M. Barnes and C. M. Rochman, *Science*, 2020, **369**, 1515.
- 3 J. Barrett, Z. Chase, J. Zhang, M. M. B. Holl, K. Willis, A. Williams, B. D. Hardesty and C. Wilcox, *Front. Mar. Sci.*, 2020, **7**, 576170.
- 4 I. A. Kane, M. A. Clare, E. Miramontes, R. Wogelius, J. J. Rothwell, P. Garreau and F. Pohl, *Science*, 2020, **368**, 1140.
- 5 M. Cole, P. Lindeque, E. Fileman, C. Halsband, R. Goodhead, J. Moger and T. S. Galloway, *Environ. Sci. Technol.*, 2013, **47**, 6646–6655.
- 6 S. Magni, C. Della Torre, G. Garrone, A. D'Amato, C. C. Parenti and A. Binelli, *Environ. Pollut.*, 2019, **250**, 407–415.
- 7 S. Magni, F. Gagné, C. André, C. Della Torre, J. Auclair, H. Hanana, C. C. Parenti, F. Bonasoro and A. Binelli, *Sci. Total Environ.*, 2018, **631–632**, 778–788.
- 8 L. G. A. Barboza, A. Dick Vethaak, B. R. B. O. Lavorante, A.-K. Lundebye and L. Guilhermino, *Mar. Pollut. Bull.*, 2018, **133**, 336–348.
- 9 L. Li, Y. Luo, R. Li, Q. Zhou, W. J. G. M. Peijnenburg, N. Yin, J. Yang, C. Tu and Y. Zhang, *Nat. Sustainability*, 2020, **3**, 929–937.
- 10 P. Marsden, A. A. Koelmans, J. Bourdon-Lacombe, T. Gouin, L. D. Anglada, D. Cunliffe, P. Jarvis, J. Fawell and J. D. France, *Microplastics in drinking water*, Report 9789241516198, World Health Organization, Geneva, 2019.
- 11 L. M. Hernandez, E. G. Xu, H. C. E. Larsson, R. Tahara, V. B. Maisuria and N. Tufenkji, *Environ. Sci. Technol.*, 2019, **53**, 12300–12310.
- 12 R. Hurley, J. Woodward and J. J. Rothwell, *Nat. Geosci.*, 2018, **11**, 251–257.
- 13 G.-X. Wang, D. Huang, J.-H. Ji, C. Völker and F. R. Wurm, *Adv. Sci.*, 2021, **8**, 2001121.
- 14 M. S. Bank, Y. S. Ok and P. W. Swarzenski, *Science*, 2020, **369**, 1315.
- 15 K. Duis and A. Coors, *Environ. Sci. Eur.*, 2016, **28**, 2.
- 16 A. L. Dawson, S. Kawaguchi, C. K. King, K. A. Townsend, R. King, W. M. Huston and S. M. Bengtson Nash, *Nat. Commun.*, 2018, **9**, 1001.



- 17 Editorial, *Nat. Nanotechnol.*, 2019, **14**, 299–299.
- 18 E. S. Germanov, A. D. Marshall, L. Bejder, M. C. Fossi and N. R. Loneragan, *Trends Ecol. Evol.*, 2018, **33**, 227–232.
- 19 W. K. So, K. Chan and C. Not, *Mar. Pollut. Bull.*, 2018, **133**, 500–505.
- 20 P. K. Cheung and L. Fok, *Water Res.*, 2017, **122**, 53–61.
- 21 Z. Zhang and Y. Chen, *Chem. Eng. J.*, 2020, **382**, 122955.
- 22 L. Bradney, H. Wijesekara, K. N. Palansooriya, N. Obadamudalige, N. S. Bolan, Y. S. Ok, J. Rinklebe, K.-H. Kim and M. B. Kirkham, *Environ. Int.*, 2019, **131**, 104937.
- 23 M. A. Browne, P. Crump, S. J. Niven, E. Teuten, A. Tonkin, T. Galloway and R. Thompson, *Environ. Sci. Technol.*, 2011, **45**, 9175–9179.
- 24 H. Wijesekara, N. S. Bolan, L. Bradney, N. Obadamudalige, B. Seshadri, A. Kunhikrishnan, R. Dharmarajan, Y. S. Ok, J. Rinklebe, M. B. Kirkham and M. Vithanage, *Chemosphere*, 2018, **199**, 331–339.
- 25 K. L. Law and R. C. Thompson, *Science*, 2014, **345**, 144.
- 26 D. M. Mitrano and W. Wohlleben, *Nat. Commun.*, 2020, **11**, 5324.
- 27 R. Z. Habib, M. M. Salim Abdoon, R. M. Al Meqbaali, F. Ghebremedhin, M. Elakashlan, W. F. Kittaneh, N. Cherupurakal, A. I. Mourad, T. Thiemann and R. Al Kindi, *Environ. Pollut.*, 2020, **258**, 113831.
- 28 C. A. King, J. L. Shamshina, O. Zavgorodnya, T. Cutfield, L. E. Block and R. D. Rogers, *ACS Sustainable Chem. Eng.*, 2017, **5**, 11660–11667.
- 29 J. Coombs O'Brien, L. Torrente-Murciano, D. Mattia and J. L. Scott, *ACS Sustainable Chem. Eng.*, 2017, **5**, 5931–5939.
- 30 F. Davarci, D. Turan, B. Ozcelik and D. Poncelet, *Food Hydrocolloids*, 2017, **62**, 119–127.
- 31 M. Österberg, M. H. Sipponen, B. D. Mattos and O. J. Rojas, *Green Chem.*, 2020, **22**, 2712–2733.
- 32 H. C. Nam and W. H. Park, *ACS Biomater. Sci. Eng.*, 2020, **6**, 2440–2449.
- 33 K. Gallardo, R. Castillo, N. Mancilla and F. Remonsellez, *Front. Chem. Eng.*, 2020, **2**, 4.
- 34 S. Ju, Y. Eom, S. Y. Kim, S. Y. Hwang, D. S. Hwang, D. X. Oh and J. Park, *Chem. Eng. J.*, 2020, **391**, 123493.
- 35 C. F. Hunt, W. H. Lin and N. Voulvoulis, *Nat. Sustainability*, 2021, **4**, 366–372.
- 36 N. Goyal, P. Gao, Z. Wang, S. Cheng, Y. S. Ok, G. Li and L. Liu, *J. Hazard. Mater.*, 2020, **392**, 122494.
- 37 M. Rinaudo, *Prog. Polym. Sci.*, 2006, **31**, 603–632.
- 38 T. H. Tran, H.-L. Nguyen, D. S. Hwang, J. Y. Lee, H. G. Cha, J. M. Koo, S. Y. Hwang, J. Park and D. X. Oh, *Carbohydr. Polym.*, 2019, **205**, 392–400.
- 39 S. Choi, H. Jeon, M. Jang, H. Kim, G. Shin, J. M. Koo, M. Lee, H. K. Sung, Y. Eom, H.-S. Yang, J. Jegal, J. Park, D. X. Oh and S. Y. Hwang, *Adv. Sci.*, 2021, **8**, 2003155.
- 40 L. Payet and E. M. Terentjev, *Langmuir*, 2008, **24**, 12247–12252.
- 41 V. H. Kulkarni, P. V. Kulkarni and J. Keshavayya, *J. Appl. Polym. Sci.*, 2007, **103**, 211–217.
- 42 I. Genta, M. Costantini, A. Asti, B. Conti and L. Montanari, *Carbohydr. Polym.*, 1998, **36**, 81–88.
- 43 R. Amen, H. Bashir, I. Bibi, S. M. Shaheen, N. K. Niazi, M. Shahid, M. M. Hussain, V. Antoniadis, M. B. Shakoor, S. G. Al-Solaimani, H. Wang, J. Bundschuh and J. Rinklebe, *Chem. Eng. J.*, 2020, **396**, 125195.
- 44 A. Atamaleki, M. Sadani, A. Raoofi, A. Miri, S. G. Bajestani, Y. Fakhri, Z. Heidarinejad and A. M. Khaneghah, *Trends Food Sci. Technol.*, 2020, **95**, 1–9.
- 45 Z. Han, Y. Zeng, H. Lu and L. Zhang, *Carbohydr. Res.*, 2015, **413**, 75–84.
- 46 M. L. Duarte, M. C. Ferreira, M. R. Marvão and J. Rocha, *Int. J. Biol. Macromol.*, 2002, **31**, 1–8.
- 47 S. Lee, Y. Eom, J. Park, J. Lee and S. Y. Kim, *Sci. Rep.*, 2017, **7**, 10012.
- 48 Q. Chen, Y. Liu, T. Wang, J. Wu, X. Zhai, Y. Li, W. W. Lu, H. Pan and X. Zhao, *J. Mater. Chem. B*, 2017, **5**, 3686–3696.
- 49 C. Mura, A. Nácher, V. Merino, M. Merino-Sanjuán, M. Manconi, G. Loy, A. M. Fadda and O. Díez-Sales, *Colloids Surf., B*, 2012, **94**, 199–205.
- 50 M. A. Mohammed, J. T. M. Syeda, K. M. Wasan and E. K. Wasan, *Pharmaceutics*, 2017, **9**, 53.
- 51 L. M. B. Ferreira, A. M. dos Santos, F. I. Boni, K. C. dos Santos, L. M. G. Robusti, M. P. C. de Souza, N. N. Ferreira, S. G. Carvalho, V. M. O. Cardoso, M. Chorilli, B. S. F. Cury, D. R. M. de Godoi and M. P. D. Gremião, *Carbohydr. Polym.*, 2020, **250**, 116968.
- 52 A. Y. Jee and M. Lee, *Polym. Test.*, 2010, **29**, 95–99.
- 53 Y. Yang, C.-E. He, W. Tang, C. P. Tsui, D. Shi, Z. Sun, T. Jiang and X. Xie, *J. Mater. Chem. A*, 2014, **2**, 20038–20047.
- 54 W. Li, Z. H. Zhai, Q. Pang, L. Kong and Z. R. Zhou, *Wear*, 2013, **301**, 353–361.
- 55 P. Nikaeen, D. Depan and A. Khattab, *Nanomaterials*, 2019, **9**, 1357.
- 56 D. Manas, M. Ovsik, A. Mizera, M. Manas, L. Hylova, M. Bednarik and M. Stanek, *Polymers*, 2018, **10**, 158.
- 57 G. Kaupp and M. R. Naimi-Jamal, *J. Mater. Chem.*, 2011, **21**, 8389–8400.
- 58 G. Crini and P.-M. Badot, *Prog. Polym. Sci.*, 2008, **33**, 399–447.
- 59 A. Li, R. Lin, C. Lin, B. He, T. Zheng, L. Lu and Y. Cao, *Carbohydr. Polym.*, 2016, **148**, 272–280.
- 60 M. Guo, J. Wang, C. Wang, P. J. Strong, P. Jiang, Y. S. Ok and H. Wang, *Sci. Total Environ.*, 2019, **682**, 340–347.
- 61 F. Zereini, F. Alt, J. Messerschmidt, C. Wiseman, I. Feldmann, A. von Bohlen, J. Müller, K. Liebl and W. Püttmann, *Environ. Sci. Technol.*, 2005, **39**, 2983–2989.
- 62 S. Nsereko and M. Amiji, *Biomaterials*, 2002, **23**, 2723–2731.
- 63 M. C. Rillig, *Nat. Sustainability*, 2020, **3**, 887–888.
- 64 A. A. de Souza Machado, C. W. Lau, W. Kloas, J. Bergmann, J. B. Bachelier, E. Faltin, R. Becker, A. S. Görlich and M. C. Rillig, *Environ. Sci. Technol.*, 2019, **53**, 6044–6052.
- 65 H. Kim, H. Jeon, G. Shin, M. Lee, J. Jegal, S. Y. Hwang, D. X. Oh, J. M. Koo, Y. Eom and J. Park, *Green Chem.*, 2021, **23**, 2293–2299.



- 66 N. M. El-Sawy, H. A. A. El-Rehim, A. M. Elbarbary and E.-S. A. Hegazy, *Carbohydr. Polym.*, 2010, **79**, 555–562.
- 67 X. Yuan, J. Zheng, S. Jiao, G. Cheng, C. Feng, Y. Du and H. Liu, *Carbohydr. Polym.*, 2019, **220**, 60–70.
- 68 V. Saharan, R. V. Kumaraswamy, R. C. Choudhary, S. Kumari, A. Pal, R. Raliya and P. Biswas, *J. Agric. Food Chem.*, 2016, **64**, 6148–6155.
- 69 S. G. Sparg, M. G. Kulkarni, M. E. Light and J. Van Staden, *Bioresour. Technol.*, 2005, **96**, 1323–1330.

